



Science Arts & Métiers (SAM)

is an open access repository that collects the work of Arts et Métiers Institute of Technology researchers and makes it freely available over the web where possible.

This is an author-deposited version published in: <https://sam.ensam.eu>
Handle ID: <http://hdl.handle.net/10985/15091>

To cite this version :

Soundes DJAZIRI, Dominique THIAUDIÈRE, Guillaume GEANDIER, Pierre Olivier RENAULT, Éric LE BOURHIS, P GOUDEAU, Olivier CASTELNAU, D FAURIE - Controlled biaxial deformation of nanostructured W/Cu thin films studied by X-ray diffraction - Materials Science and Engineering: A - Vol. Volume 205, Issue 5, p.1420-1425 - 2010

Any correspondence concerning this service should be sent to the repository

Administrator : scienceouverte@ensam.eu



Controlled biaxial deformation of nanostructured W/Cu thin films studied by X-ray diffraction

S. Djaziri^a, D. Thiaudière^b, G. Geandier^b, P.-O. Renault^{a,*}, E. Le Bourhis^a, P. Goudeau^a, O. Castelnau^c, D. Faurie^d

^a Institut P', CNRS-Université de Poitiers-ENSMA, UPR 3346, 86962 Futuroscope, France

^b Synchrotron SOLEIL, L'Orme des Merisiers, BP 48, 91192 Gif sur Yvette, France

^c Laboratoire PIMM, ENSAM, 151, Boulevard de l'Hôpital, 75013 Paris, France

^d LPMTM, UPR 9001 CNRS, Université Paris-Nord, 93430 Villetaneuse, France

ARTICLE INFO

Keywords:

X-ray diffraction
Mechanical behaviour
Thin film
Nanocomposite
Biaxial deformation

ABSTRACT

The deformation behaviour of 150 nm thick W/Cu nanocomposite deposited on polyimide substrates has been analysed under equi-biaxial tensile testing coupled to X-ray diffraction technique. The experiments were carried out using a biaxial device that has been developed for the DiffAbs beamline of SOLEIL synchrotron source. Finite element analysis has been performed to study the strain distribution into the cruciform shape substrate and define the homogeneous deformed volume. X-ray measured elastic strains in tungsten sub-layers could be carried out for both principal directions. The strain field was determined to be almost equi-biaxial as expected and compared to finite element calculations.

1. Introduction

The continued interest in nanostructures over the past decades is due to the fact that electronic, optical, mechanical and magnetic properties may differ from those of their bulk counterparts [1] and also to their wide range of applications in various fields. In particular, thin metal films on polymer substrates are in use in many technological applications, based on stretchable microelectronics [2,3] and polymer metallization [4]. In aeronautics, metal/polymer composites are very interesting because of their mechanical flexibility, light weight and low thickness. The combination of different materials in form of nanolayered systems are known to improve the mechanical properties of thin coatings [5]. Noticeably, the combination of the high thermal conductivity of copper (Cu) and the low thermal expansion coefficient of tungsten (W) makes W-Cu composites attractive for thermal management applications [6]. In addition to their electrical properties, these metal composites present interesting mechanical strength resulting from the compromise between the high strength of W and the ductility of Cu [7]. Nevertheless, during fabrication and service, large mechanical stresses may develop and lead to mechanical failure (cracking and delamination). These stresses result from deposition process, microstructural changes, thermal mismatch, or external loading during

service. Therefore, understanding mechanical properties of thin films is essential for ensuring the reliability of such structures. Tensile testing coupled to X-ray diffraction (XRD) has been widely employed as a method for studying the mechanical behaviour of supported metal thin films [8–14]. Uniaxial tensile testing commonly used imposes a biaxial stress state with a transversal component that is determined by Poisson's ratio mismatch between the substrate and the deposited film [15]. In order to control both stress components and then mimic realistic loadings, we have developed within the framework of an ANR project (2005–2009) a unique biaxial tensile machine for synchrotron measurements and for this kind of samples. Noticeably, bulge and ring on ring tests can be used to investigate the behaviour of thin films under plane stresses [16–18]. Due to the thermal expansion mismatch between film and substrate, a stress states can also be applied to the film by annealing the thin film/substrate set at elevated temperatures [19–21]. However, these techniques are restricted to equi-biaxial loading. Our new tensile device allows both equi-biaxial loading and controlled non-equi-biaxial loading. This machine is now available and optimized at the DiffAbs beamline of the French synchrotron radiation facility (SOLEIL, Saint Aubin) thanks to *in-situ* controlled biaxial tests on W thin films [22]. Synchrotron XRD allows faster and more accurate measurements on small diffracting volumes of material with high resolution [23] compared to laboratory setup using conventional X-ray sources. In this paper, we present the latest results of *in-situ* tests carried out on W/Cu multilayered thin films deposited onto a polyimide cruciform substrate.

* Corresponding author.

E-mail address: pierre.olivier.renault@univ-poitiers.fr (P.-O. Renault).

2. Experimental

2.1. The biaxial tensile machine

The tensile machine has been designed to allow for loading along two normal axes cruciform substrates coated by the studied films. A polymeric substrate with a low elastic modulus (around 3 GPa) is chosen to optimize the stress concentration in metallic films having higher elastic modulus (around 400 GPa for W). Here we used 125- μm -thick polyimide substrate (sofimide® from MICEL). Fig. 1 shows the machine installed in DiffAbs-SOLEIL beamline with a centre-coated specimen.

The machine is composed of four identical module components. Each module contains a motor, a force sensor and a cylindrical fixation. The weight of the device is 3.5 kg and its size is $19 \times 19 \times 8.5 \text{ cm}^3$ with a free space at the centre. The machine can apply loads up to 200 N. The cruciform substrates were coated at their centre only and gripped by a cam rotating in the cylinder fixation.

2.2. Finite elements (FE) design and modelling of the substrate

The use of this new experimental set-up requires the design of the cruciform specimen geometry. In order to achieve homogeneous stress condition on a few square millimetres, the specimen geometry is optimised based on FE-simulation. Indeed, the required substrate geometry must allow obtaining small deformations (to study the elastic domain) within an area of the specimen centre wide enough to achieve XRD measurements. We have to keep in mind that the X-ray beam size can be of about $1 \times 1 \text{ mm}^2$ and, thus the irradiated area can be about 5 times larger. The mechanical behaviour of the polyimide cruciform substrate has been modelled using the software CAST3M (from the French atomic energy commission CEA in french). The branches of the chosen specimen are 20 mm in width and 5 mm toe weld as illustrated in Fig. 2.

Two-dimensional FE-calculations were performed under plane stress conditions because of the specimen's small thickness. The element type used for this study was triangular with 6 nodes and the central area was meshed finer than the rest of the structure. A linear elastic behaviour was adopted to assess the mechanical behaviour of the cruciform substrate biaxially loaded. This represents a good approximation of the real behaviour of the specimen since small strains involve, in general, linear stress-strain relation as experimentally determined in tensile tests. Actually, strain measurements by

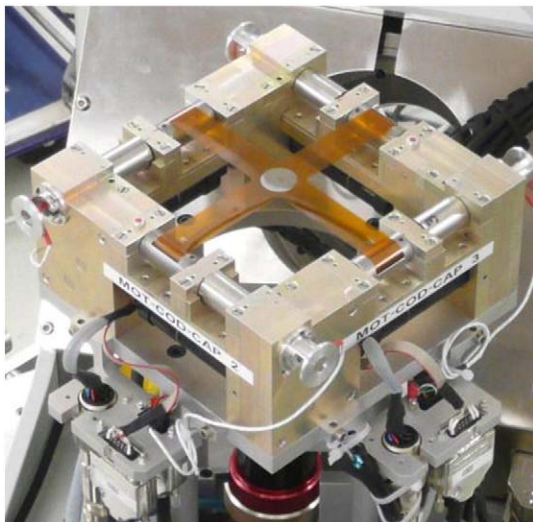


Fig. 1. Photography of the biaxial tensile machine with a gripped cruciform specimen. The W/Cu thin film can be seen at the centre of the sofimide substrate.

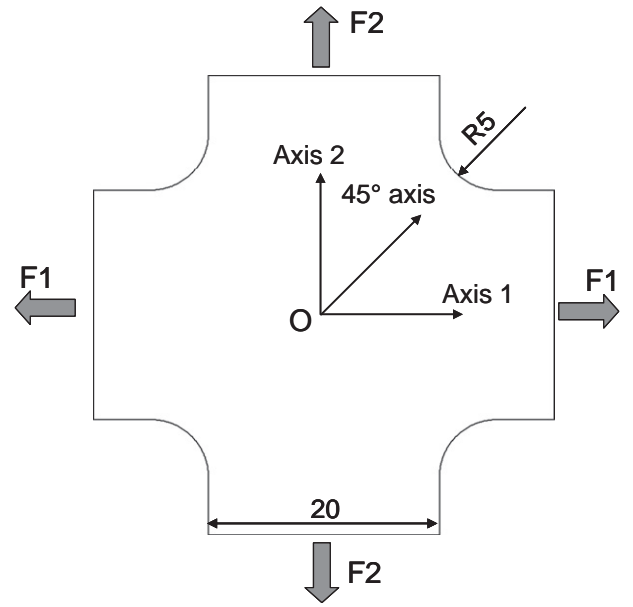


Fig. 2. Schematic representation of the cruciform substrate (only the central part in which the point O presents the structure centre), dimensions are in mm.

digital image correlation for sofimide® revealed a polynomial form of the stress-strain curves as reported by D. Y. W. Yu and F. Spaepen for a similar polyimide (supplied by Dupont de Nemours and named Kapton®) [24]. However, the behaviour is linear up to a strain of 0.8%, a value below which the experimental study was carried out. Young's modulus (E_s) and Poisson's ratio (ν_s) were determined to be $E_s = 2.7 \pm 0.1 \text{ GPa}$ and $\nu_s = 0.34$ respectively in this deformation range, values that were used in FE-calculations.

The strain distributions of the two components ε_{11} and ε_{22} in the specimen centre (on which the metal thin film is deposited) under a 50 N equi-biaxial loading are illustrated in Fig. 3a and b respectively. Due to the symmetry of the specimen, those two figures are the same by a rotation of 90° . The centre of the specimen seems to exhibit a region in which the strain is homogeneous. This is checked thanks to sections along three different axes (Fig. 2). Strain components along the axis at 45° are equal and remain constant on a distance larger than 6 mm (Fig. 4a). Along axes 1 and 2, the distance reduces to 4 mm. As shown in Fig. 4b, the strain components along axis 1 (at the right of the figure) are equal for roughly 2 mm in distance. Similarly, they are equal for a distance of 2 mm along axis 2 (at the left of the figure). Hence, the strain field can be considered as uniform in the centre of the cruciform specimen over a distance of 4 mm. We conclude, according to the FE analysis, that for a 50 N equi-biaxial loading, a 0.34% homogeneous strain is generated in a central area of 4 mm in radius. It is worth to be noted that FE calculations have been performed onto bare polyimide substrate. The thin film may modify the strain field in the substrate. Keeping in mind that the total film thickness is only 150 nm and by using a simple bi-layer elastic model, the influence of the coating on the total strain field can be estimated to be about 7–8%. This is the reason why we assume that the FE strain calculations of the bare substrate are representative of the strains in the coated substrate.

2.3. Sample preparation and characterization

The samples have been prepared and their structure has been characterized at the University of Poitiers. The *in-situ* tensile tests were carried out at SOLEIL synchrotron facility on W/Cu thin films.

The W/Cu multilayer thin films were produced at room temperature by physical vapour deposition (PVD) with an Ar^+ -ion-gun

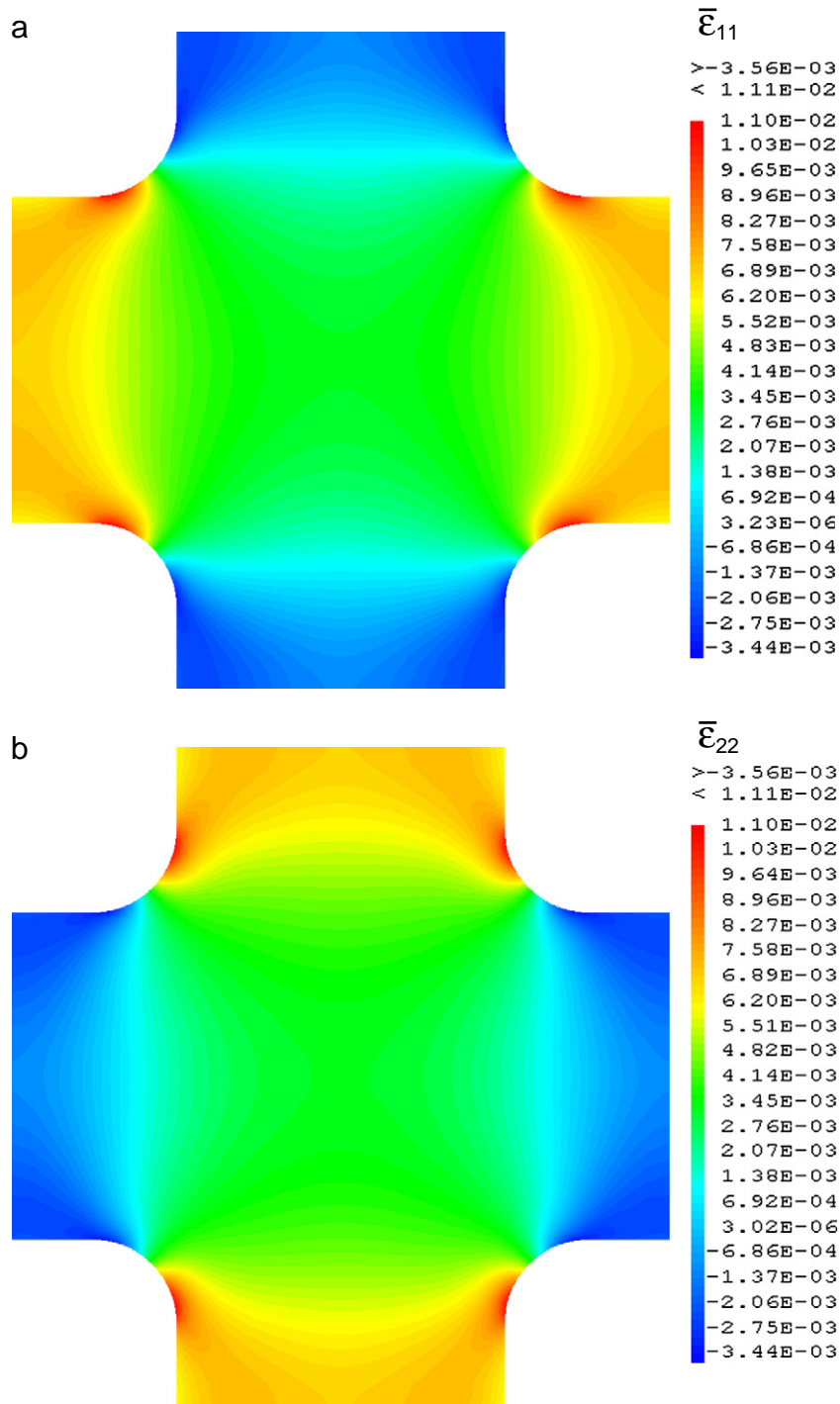


Fig. 3. FE strain field of a cruciform substrate under a 50 N equi-biaxial loading a) ϵ_{11} and b) ϵ_{22} .

sputtering beam at 1.2 keV on a 125- μm -thick cruciform polyimide substrate (sofimide® from MICEL). The base pressure of the deposition chamber was 7×10^{-5} Pa while the working pressure during film growth was approximately 10^{-2} Pa. The system investigated here comprises 37 periods of 4 nm each, composed of 3 nm W and 1 nm Cu. The total film thickness was evaluated to be about 150 nm. Texture analysis was carried out using XRD and it was shown that W crystallites of W/Cu composites exhibits a strong $\{110\}$ -fibre texture. Global residual stress determined by Stoney curvature method was -1.5 GPa while in grain W stress analysed by XRD using the $\sin^2\psi$ method was -4 GPa.

2.4. In-situ tensile testing on W/Cu film

The biaxial tensile machine is installed on the 6 circle diffractometer at the Diffabs-SOLEIL beamline. The X-ray energy and beam size have been set to 8 keV and $0.3(V) \times 1(H)$ mm² respectively. Several equi-biaxial loadings (labelled as TX where X referred to the number of the tensile loading) were applied to the composite thin film/substrate (forces in N: 9.60, 14.75, 24.40, 34.50, 39.80 and 44.50). The first applied load (9.60 N in the present case) is required for the installation of the specimen to avoid sample drift during the increase of the applied load. Thanks to the specimen size, this force does not

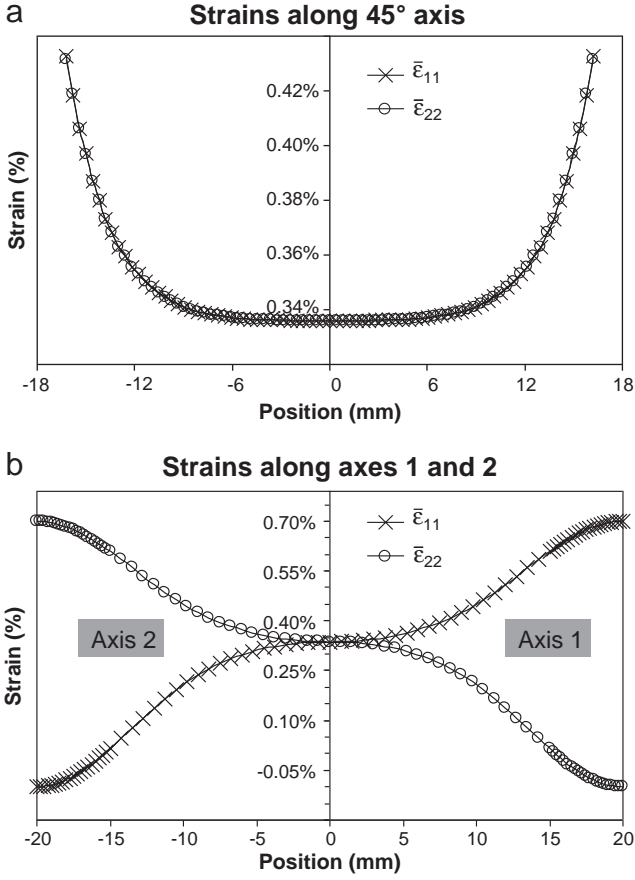


Fig. 4. FE strain components variations under a 50 N equi-biaxial loading (i.e. sections of Fig. 3) along a) 45° axis, b) axes 1 and 2 defined in Fig. 2 (the origin of the x-axis in the two figures represents the structure centre).

generate high deformations especially in the central part (about 0.06% from FE analysis). Moreover, this state allows X-ray reflectometry measurements because the specimen surface becomes flat with loading. Intra-granular strains were obtained by detecting the diffraction peaks positions shifts for each applied load. X-ray diffraction measurements have been performed only for W constituent because diffracting volume of Cu constituent is too small for reliable XRD data analysis in a reasonable experimental time

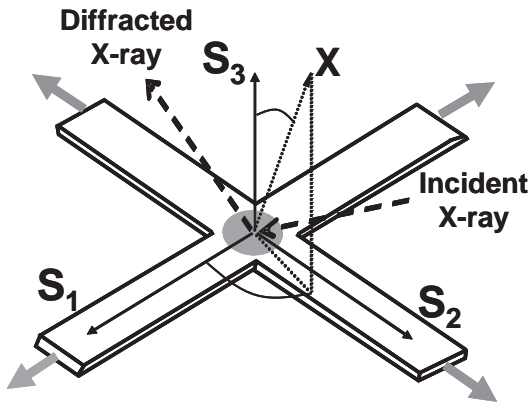


Fig. 5. Experimental configuration used for the *in-situ* tensile tests. ψ is the angle between the specimen surface normal S_3 and the diffracting plane normal. ϕ is the rotation angle of the specimen around its surface normal. S_1 and S_2 are the loading directions.

acquisition. The measurements have been performed for five different ψ angles and along two normal directions $\phi = 0^\circ$ and $\phi = 90^\circ$ (Fig. 5).

Diffraction measurements were performed on {211} crystallographic planes of W which correspond to the best compromise between high Bragg diffraction angle and strong peak intensity. Indeed, the higher 2θ angles are, the better the accuracy on strains is.

3. Results and discussion

We employ in the following the logarithm strain usually (and correctly) approximated by the engineering strain in the elastic domain. The lattice strain ε_{hkl} corresponding to a {hkl} diffracting planes is given by:

$$\varepsilon_{hkl} = \ln\left(\frac{d_{hkl}}{d_{hkl}^{(0)}}\right) = \ln\left(\frac{\sin\theta_{hkl}^{(0)}}{\sin\theta_{hkl}}\right) \approx -\cotan(\theta) \cdot \Delta\theta \quad (1)$$

where $d_{hkl}^{(0)}$ is the reference lattice spacing and $\theta_{hkl}^{(0)}$ is the associated reference diffracting angle. In the present case, the corresponding reference loading is the first loaded state, i.e. 9.60 N. d_{hkl} and θ_{hkl} are the lattice spacing and the scattering angle respectively for the loaded states. In-grain elastic strain measured by XRD depends on {hkl} planes orientation defined by the in-plane azimuth angle ϕ and the tilt angle ψ (Fig. 5).

For a non-equi-biaxial loading and for non-textured materials, the measured strains along the two axes corresponding to the two directions $\phi = 0^\circ$ and $\phi = 90^\circ$ can be written respectively as [25]:

$$\varepsilon_{0,\psi} = \frac{1}{2} S_2^{hkl} \bar{\sigma}_{11} \sin^2\psi + S_1^{hkl} (\bar{\sigma}_{11} + \bar{\sigma}_{22}) \quad (2a)$$

$$\varepsilon_{90,\psi} = \frac{1}{2} S_2^{hkl} \bar{\sigma}_{22} \sin^2\psi + S_1^{hkl} (\bar{\sigma}_{11} + \bar{\sigma}_{22}) \quad (2b)$$

where $\bar{\sigma}_{11}$ and $\bar{\sigma}_{22}$ are the macroscopic stresses applied to the thin film, $\frac{1}{2} S_2^{hkl}$ and S_1^{hkl} are the X-ray elastic constants (XECs) [25,26]. Mechanical grain interaction models such as Reuss, Voigt and the self-consistent scheme are commonly used to calculate the XECs [26]. In the case of a locally isotropic material such as W, all the mechanical models leads to the same values for X-ray elastic constants, and we can write that $\frac{1}{2} S_2^{hkl} = \frac{1+\nu}{E}$ and $S_1^{hkl} = -\frac{\nu}{E}$ where E is the Young's modulus and ν the Poisson's ratio of the material.

Moreover, when the loading is equi-biaxial ($\bar{\sigma}_{11} = \bar{\sigma}_{22} = \bar{\sigma}$), the strains along the two mentioned axes reduce to:

$$\varepsilon_\psi = \left(\frac{1+\nu}{E}\right) \bar{\sigma} \sin^2\psi - \frac{2\nu}{E} \bar{\sigma} \quad (2c)$$

These expressions reflect the $\sin^2\psi$ law which describes a linear relationship between strain versus $\sin^2\psi$ which is characteristic of macroscopically isotropic materials.

Elastic applied strains measured by XRD are plotted as a function of $\sin^2\psi$ (Fig. 6). Only the applied elastic strain is reported on Fig. 6, i.e. the total elastic strain minus the residual elastic strain. All curves are linear as expected for a locally isotropic material such as W even if it is textured [15,26]. The $\varepsilon - \sin^2\psi$ plots of Fig. 6a and b are similar. Thus we observed similar elastic strains along both directions ($\phi = 0^\circ$ and $\phi = 90^\circ$) as expected for an equi-biaxial loading. Besides, all straight lines intersect at a point close to zero strain which allows determining Poisson's ratio ν of the W constituent. This point is related to a specific sample inclination, ψ^* angle, where $\sin^2\psi^* = \frac{2\nu}{1+\nu}$. The obtained value of Poisson's ratio is around 0.29 ± 0.02 for $\phi = 0^\circ$ and around 0.28 ± 0.03 for $\phi = 90^\circ$. Those values are in good agreement with the Poisson's ratio of the bulk W (0.285). Extracting the slopes and intercepts of $\varepsilon - \sin^2\psi$ curves (Fig. 6a and b), we can determine the three principal components of the strain tensor. Indeed, the X-ray strains along the two normal axes can be written as $\varepsilon_{0,\psi} = (\bar{\varepsilon}_{11} - \bar{\varepsilon}_{33}) \sin^2\psi + \bar{\varepsilon}_{33}$ for $\phi = 0^\circ$ and

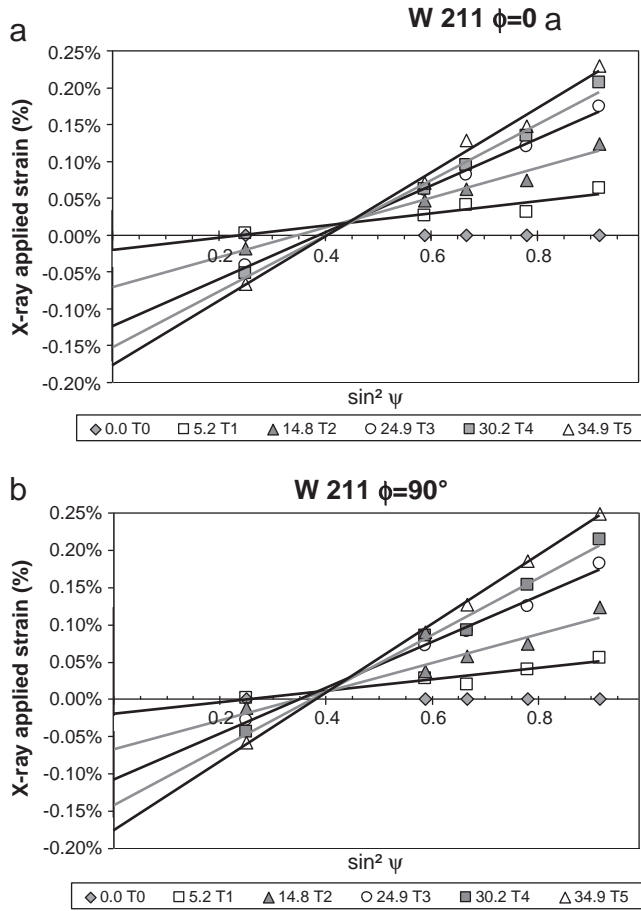


Fig. 6. X-ray applied strain as a function of $\sin^2 \psi$ for a) $\phi = 0^\circ$ and b) $\phi = 90^\circ$ i.e. along S_1 and S_2 respectively. The different equi-biaxial loading increments are labelled as TX where X referred to the number of the tensile loading. T0 is the reference loading state, T1 is the first applied loading increment (5.2 N), T2 the second (14.8 N), and so on.

$\varepsilon_{90,\psi} = (\bar{\varepsilon}_{22} - \bar{\varepsilon}_{33}) \sin^2 \psi + \bar{\varepsilon}_{33}$ for $\phi = 90^\circ$, where ε_{11} , ε_{22} and ε_{33} are the principal macroscopic strains components.

Thus, in the case of an equi-biaxial loading, ε_{11} and ε_{22} are equal to the sum of the slope and intercept of $\varepsilon - \sin^2 \psi$ curves as shown in Fig. 7a and b corresponding to the measured strain along $\phi = 0^\circ$ and $\phi = 90^\circ$ respectively.

The X-ray elastic strain values for an incremental load of $\Delta F = 50$ N can be extrapolated from Fig. 7a and b, we found values of 0.33% for $\phi = 0^\circ$ and of 0.37% for $\phi = 90^\circ$. These values are in relatively good agreement with the strain values predicted by FE analysis, i.e. 0.34% biaxial strains (see Section 3). These results show that a complete strain transfer can be assumed through the interface between the polyimide substrate and the metallic thin composite film within the elastic domain as shown recently for homogeneous thin films under uniaxial tensile loading [27]. In comparison to the pure W thin film, it appears that the incorporation of Cu into a W matrix does not affect the W phase behaviour as long as the studied domain remains in the elastic regime.

4. Conclusions

A novel biaxial machine has been developed at SOLEIL synchrotron and used for tensile testing of supported thin films in combination with XRD. Finite Element analysis showed that this device allows inducing a biaxial uniform strain field in the centre of the coated cruciform substrate over a surface of about 4×4 mm² where *in-situ* diffraction experiments have been carried out. The results obtained by

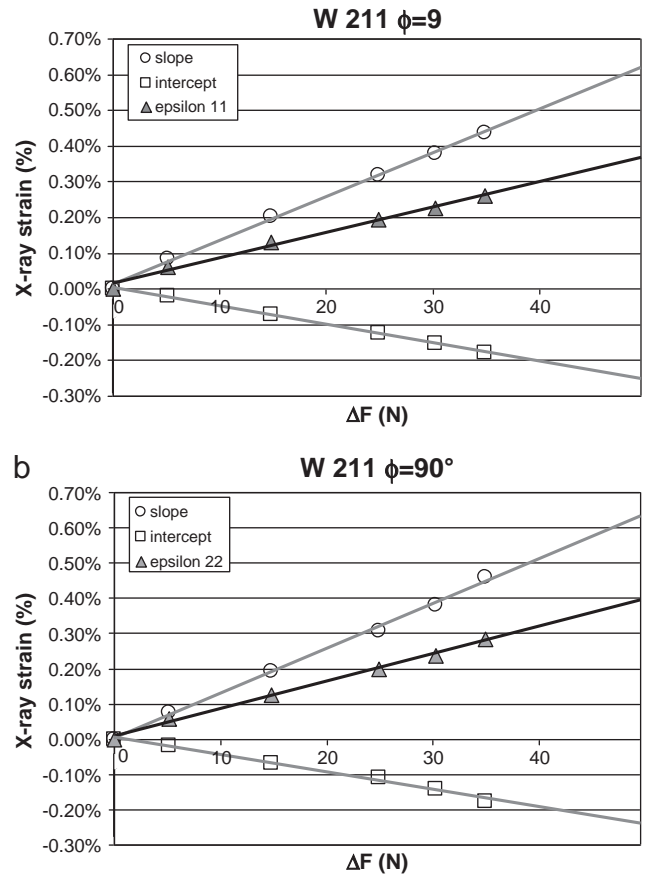


Fig. 7. X-ray strain as a function of the load applied to the cruciform specimen for a) $\phi = 0^\circ$ and b) $\phi = 90^\circ$.

studying W/Cu composite films allowed verifying the homogeneity of the equibiaxially strained zone and characterizing the elastic behaviour of nanostructured thin films (under equi-biaxial loading). The measured XRD elastic strains in W sublayers match rather well the global strain calculated by the FE analysis. Further work will include more complex loading history comprising non equi-biaxial loading and additional X-ray techniques such as reflectometry to investigate the tungsten/copper period and thus the mechanical response of the composite at different scales. In addition, X-ray absorption spectroscopy could be used to study local order in copper clusters since this phase does not give any diffraction pattern. In situ measurements during loading will allow following strains in copper.

References

- [1] F. Spaepen, D.W.Y. Yu, *Scr. Mater.* 50 (2004) 729.
- [2] M.A. Meyers, A. Mishra, D.J. Benson, *Prog. Mater. Sci.* 51 (2006) 427.
- [3] S.P. Lacour, D. Chan, S. Wagner, T. Li, Z. Suo, *Appl. Phys. Lett.* 88 (2006) 204103.
- [4] W.T. Li, R.B. Charters, B. Luther-Davies, L. Mar, *Appl. Surf. Sci.* 233 (2004) 227.
- [5] P.A. Gruber, E. Arzt, R. Spolenak, *J. Mater. Res.* 24 (2009) 1906.
- [6] A. Luedtke, *Adv. Eng. Mater.* 6 (2004) 142.
- [7] P.M. Geffroy, T. Chartier, J.F. Silvain, *Ann. Rev. Mater. Sci.* 9 (2007) 547.
- [8] P.-O. Renault, K.F. Badawi, L. Bimbault, Ph. Goudeau, E. Elkaim, J.P. Lauriat, *Appl. Phys. Lett.* 73 (1998) 1952.
- [9] O. Kraft, M. Hommel, E. Arzt, *Mater. Sci. Eng., A* 288 (2000) 209.
- [10] K.F. Badawi, P. Villain, Ph. Goudeau, P.-O. Renault, *Appl. Phys. Lett.* 80 (2002) 4705.
- [11] D. Faurie, P.O. Renault, E. Le Bourhis, Ph. Goudeau, O. Castelnau, R. Brenner, G. Patriarche, *Appl. Phys. Lett.* 89 (2006) 061911.
- [12] I.C. Noyan, G. Sheikh, *J. Mater. Res.* 8 (1992) 8.
- [13] A. Kretschmann, W.-M. Kuschke, S.P. Baker, E. Arzt, *Mater. Res. Soc. Symp. Proc.* 436 (1996) 59.
- [14] I.C. Noyan, G. Sheikh, *Mater. Res. Soc. Symp. Proc.* 308 (1993) 3.
- [15] D. Faurie, P.-O. Renault, E. Le Bourhis, Ph. Goudeau, *Acta Mater.* 54 (2006) 4503.

- [16] S. Eve, N. Hubert, O. Kraft, A. Last, D. Rabus, M. Schlagenhof, *Rev. Sci. Instr.* 77 (2006) 103902.
- [17] J.J. Vlassak, W.D. Nix, *J. Mater. Res.* 7 (1992) 3242.
- [18] O.R. Shojaei, A. Karimi, *Thin Solid Films* 332 (1998) 202.
- [19] G. Cornella, S.-H. Lee, W.D. Nix, J.C. Bravman, *Appl. Phys. Lett.* 71 (1997) 2949.
- [20] S.P. Baker, A. Kretschmann, E. Arzt, *Acta Mater.* 49 (2001) 2145.
- [21] J. Keckes, *J. Appl. Cryst.* 38 (2005) 311.
- [22] G. Geandier et al., *Rev. Sci. Instr.* (in press).
- [23] D. Faurie, P.O. Renault, E. Le Bourhis, P. Villain, Ph. Goudeau, F. Badawi, *Thin Solid Films* 201 (2004) 469.
- [24] D.W.Y. Yu, F. Spaepen, *J. Appl. Phys.* 95 (2004) 2991.
- [25] V. Hauk, *Structural and Residual Stress Analysis by Non destructive Methods: Evaluation, Application, Assessment*, Elsevier, Amsterdam, 1997.
- [26] D. Faurie, O. Castelnau, R. Brenner, P.-O. Renault, E. Le Bourhis, Ph. Goudeau, *J. Appl. Cryst.* 42 (2009) 1073.
- [27] G. Geandier, P.-O. Renault, E. Le Bourhis, Ph. Goudeau, D. Faurie, C. Le Burlot, Ph. Djémia, O. Castelnau, S.M. Chérif, *Appl. Phys. Lett.* 96 (2010) 041905.